Theoretical and Applied Fracture Mechanics 92 (2017) 381–393

Contents lists available at ScienceDirect

Theoretical and Applied Fracture Mechanics

journal homepage: www.elsevier.com/locate/tafmec

Development of a strain based fracture assessment procedure for undermatched pipe girth welds subjected to bending

Rodolfo F. de Souza *, Claudio Ruggieri

Department of Naval Architecture and Ocean Engineering, University of São Paulo, São Paulo, Brazil

ARTICLE INFO

Article history:
Received 15 March 2017
Revised 12 July 2017
Accepted 13 July 2017
Available online 27 July 2017

Keywords:
Strain based analysis
J-integral
Weld strength mismatch
Girth weld
Reeling
Steel catenary risers
Structural integrity assessment

ABSTRACT

Structural integrity assessment of pipeline girth welds subjected to high strain levels which arises from the reel-lay method relies on precise crack driving force estimation procedures. Recent developments in subsea technology favor the use of high strength carbon steel pipelines with an internal corrosion resistant layer to increase protection against corrosive fluids. In contrast to homogeneous structural components, the bimetal configuration may induce the occurrence of weld strength undermatch, with a strong impact on the relationship between remote applied load and crack tip constraint. This work explores the development of a crack driving force estimation procedure based on a strain-based version of the EPRI *J* estimation scheme coupled with the equivalent stress-strain relationship method (ESSRM) and a weld geometry simplification procedure. The proposed framework takes advantage of the displacement controlled nature of the reeling process. Extensive 3D analyses provide a large set of fracture parameters applicable to the strain-based EPRI methodology followed by parametric analyses conducted to assess the accuracy of the new procedure. Subsequently, a case study is performed to determine the tolerable crack sizes in an idealized pipe installation. The procedure shows an overall good agreement to the benchmark analyses and increased accuracy when compared to the recommended approach proposed by DNV.

1. Introduction

Offshore pipeline installation by the reel-lay method has become widely employed by the oil and gas industry in recent years. This method allows the pipeline fabrication and inspection to be performed onshore, in contrast to the traditional S-lay and J-lay pipe laying techniques [1]. After welding, the pipeline is coiled around a large diameter reel on a vessel and transported to the sea where the pipe is unreeled, straightened and finally deployed to the seafloor as illustrated in Fig. 1. While fast and cost effective, the reeling process may subject the pipeline to global strain levels above the elastic limit of the material with a potentially strong impact on the structural integrity assessment of the pipe girth weld.

The increasing demand for energy has motivated the exploration and production of oil and gas in more hostile environments (including deep water reservoirs), thus motivating the introduction of new engineering techniques. Among the technologies employed in recent oil field developments, the bimetal pipes (clad/lined pipes) represent a case of considerable interest [2]. Here, a C-Mn steel pipe with a internal layer of corrosion resistant alloy (CRA) is adopted to guarantee the required resistance against corrosion [2–4]. Despite being an economically viable option, the use of clad/lined pipes produces a dissimilar girth weld with different mechanical properties than those corresponding to the external pipe material as the consumable employed in the welding process has the same properties of the CRA metal.

Engineering critical assessment (ECA) methodologies currently recommended by structural integrity standards (e.g. DNV-OS-F101 [5], BS7910 [6], API579 [7]) are essentially developed for load controlled conditions. Although effective for a wide variety of cases, they do not necessarily provide accurate assessments for pipes under displacement controlled bending undergoing large scale plasticity. Tkaczyk et al. [8] have demonstrated that traditional ECA methodologies may lead to inaccurate fracture assessments for reeled pipelines and, thus, several assumptions and safety factors should be applied to elevate the crack driving forces therefore ensuring conservative tolerable defect sizes.

The dissimilar weld configuration is another major concern and key issue in structural integrity assessment procedures. While current standards recommend a weld filler metal that overmatches the parent metal properties, the girth weld fabricated with a corrosion resistant alloy usually has lower yield strength (and, presum-

* Corresponding author.
E-mail address: rofigueira.souza@usp.br (R.F. Souza).

https://doi.org/10.1016/j.tafmec.2017.07.012
0167-8442/

Nomenclature

α	dimensionless parameter of the Ramberg–Osgood model
$\bar{\epsilon}$	logarithmic strain
$\bar{\sigma}$	uniaxial true stress
β	weld groove angle
ϵ_{ys}	yield strain
ν	Poisson's ratio
ψ	slenderness parameter
$\sigma_{bm}(\varepsilon_p)$	stress-plastic strain relationship of the base material
σ_{bw}	yield stress of the base material
$\sigma_{eq}(\varepsilon_p)$	equivalent stress-plastic strain relationship
$\sigma_{wm}(\varepsilon_p)$	stress-plastic strain relationship of the weld material
σ_{ys}	yield stress
σ_{yw}	yield stress of the weld material
θ	surface crack length
ε_z	global applied strain
φ	angle of rotation imposed in the reference point
a	crack depth
b	remaining crack ligament
c	circumferential crack half-length
D_e	pipe (cylinder) outer diameter
E', E	Young's modulus under plane stress (plane strain) conditions
f_1	functions of the weld joint geometry and mismatch ratio
f_2	functions of the weld joint geometry and mismatch ratio
g_1	dimensionless proportionality parameter between J_p and applied strain
h_{eq}	width of the equivalent square weld bevel
h_r	root width
J	J-integral
K_I	(Mode I) elastic stress intensity factor
L	pipe model length
M	applied bending moment
M_y	weld strength mismatch
M_0	limit load of the cracked pipe configuration
M_0^{bm}	limit bending load of the homogeneous structure
M_0^{mism}	limit bending load of the idealized bi-material welded joint
n	Ramberg-Osgood strain hardening exponent
N_0^{bm}	limit tension load of the homogeneous structure
N_0^{mism}	limit tension load of the idealized bi-material welded joint
P_0^{bm}	limit load for the homogeneous component made of the base material
P_0^{mism}	limit load of the idealized bi-material welded joint
R-squared	coefficient of determination
R_b	reel drum radius
R_m	mean radius of pipe
t	pipe wall thickness
CDF	crack driving forces
CRA	corrosion resistant alloy
CTOD	crack tip opening displacement
ECA	engineering critical assessment
EPRI	electric power research institute
ESSRM	equivalent stress-strain relationship method
FEA	finite element analysis
FFS	fitness-for-service
PFiniteC	Finite circumferential part-through surface internal cracks at the girth weld of pipelines subjected to tension load
SCR	steel catenary riser
SGC	small geometry change

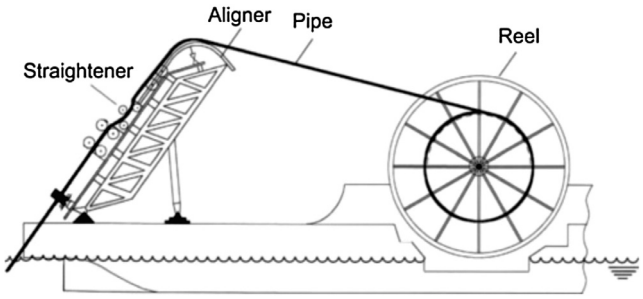

Fig. 1. Illustration of the reeling process [1].

ably, higher strain hardening behavior) than the carbon steel outer pipe (undermatch) [4]. The strength mismatch among metal properties alters the deformation pattern at the crack tip with a potentially strong impact on the relationship between remote loading and crack tip constraint [9,10].

The effectiveness of defect assessment procedures depends on accurate descriptions of crack driving forces (CDF), characterized in terms of the J-integral or the crack tip opening displacement (CTOD). The need of more precise CDF solutions for reeled pipelines has motivated the development of different estimation procedures for this class of structural components. Tkaczyk et al. [8] and Chiodo and Ruggieri [11] have published a set of CDF solutions following a stress-based methodology for a wide range of cracked pipe configurations applicable to homogeneous materials. While these procedures show better accuracy than traditional techniques, they do not take into account the displacement controlled nature of the reeling process, where global strain applied in the structure can be directly calculated from the geometry of the pipe and the reel drum radius, without being necessary to know the bending moment *vs.* strain relationship, as required by previous works. Another advantage of the strain-based fracture approach for reeled pipelines is the approximately linear evolution of the CDF *vs.* applied strain in the pipe, as reported by Østby et al. [12], and schematically shown in Fig. 2. While the CDF follows a linear evolution over the strain range, it has a more complex behavior when it is determined as a function of bending moment: it is almost linear at low strains and then increases sharply at typical reeling deformation levels (2–3%). Here, even small changes in the applied bending moment can lead to larger differences in the corresponding estimate of the CDF thereby adversely impacting the specification of tolerable defect sizes.

Nourpanah and Taheri [13] developed CDF estimation equations based on a displacement controlled approach to assess fracture behavior in reeled pipelines and subsequently Parise et al. [14] proposed a strain-based version of the EPRI framework [15] which allows its direct extension to displacement controlled conditions. In spite of the evident advances in these works, such procedures either are only applicable to CDF estimations in structural components made of homogeneous materials or present limitations that reduce its applicability range. Moreover, fracture assessment of welded joints cannot be performed in a straightforward

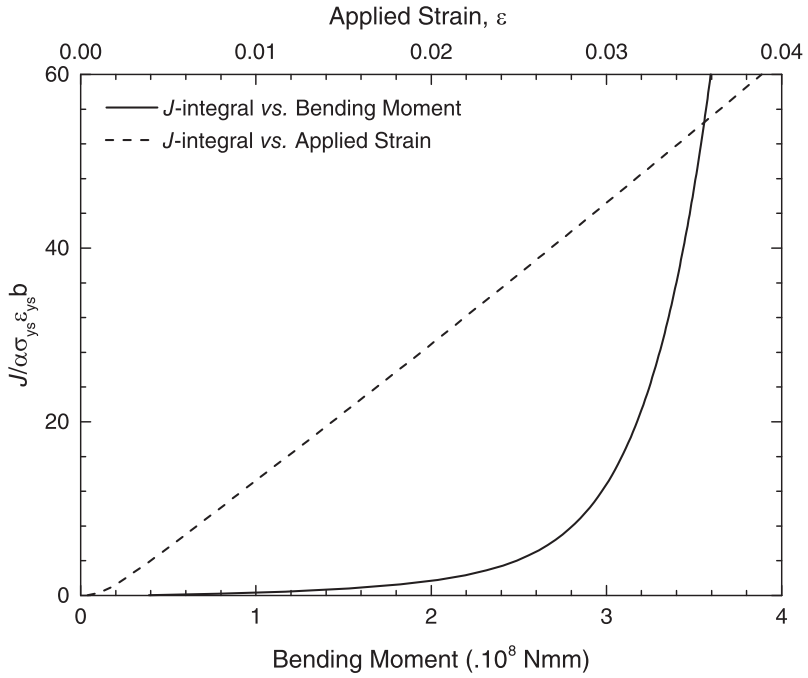

Fig. 2. Evolution of *J*-integral against applied bending moment and axial strain for a typical cracked pipe.

manner as traditional techniques developed for homogeneous components.

Inclusion of weld strength mismatch in CDF evaluation has been investigated by several authors. In the seminal work of Lei and Ainsworth [16,17], a *J*-integral evaluation procedure for welded joints is proposed using the concept of an equivalent stress and strain curve. In the specific case of reeling, Østby [18] has recently reported a CTOD estimation scheme based on the linear relationship between CDF and applied strain, where effects of weld strength mismatch are included by means of an effective defect depth which includes the influence of material heterogeneity. Recently, Pepin et al. [4] extended that methodology to analyze undermatched welds and materials with yield plateau.

Zhang et al. [19] published a CDF estimation scheme for embedded and external surface cracks including the clad layer thickness for a limited number of weld and clad material properties. Using an alternative strategy, SINTEF [2] reported a new assessment approach for clad and lined pipes based on shell and line-spring finite elements, in which a procedure to estimate the equivalent stress-strain curve for a three material configuration is adopted.

Bonora et al. [20,21] have investigated a new fracture assessment for inner, outer and embedded flaws in clad pipes with partial overmatch, considering a welded zone with three distinct material properties (clad, weld and base metal). Crack driving forces have been evaluated using an equivalent stress-strain curve derived from the lower bound properties of such materials. Verification analyses showed that application of this definition for the equivalent material response provides good agreement with finite element solutions considering the multi-material configuration.

More recently, Souza and Ruggieri [3] and Paredes and Ruggieri [22] developed a *J*-integral estimation scheme for cracks at the girth weld based on a modification of the EPRI methodology to include the effects of weld strength mismatch and a simplified procedure to consider the weld groove geometry.

The objective of this study is to investigate the application of a strain-based version of the EPRI methodology (see [14,15]) coupled with a weld bevel simplification procedure and the equivalent stress-strain relationship (ESSRM) for the analysis of circumferential surface part-through cracks in undermatched girth welds of clad and lined pipes under bending load. The investigation includes a detailed description of the crack driving force procedure and extensive 3D numerical analyses of a wide range of cracked pipe configurations. A parametric study is performed to verify the accuracy of crack driving force estimations. Finally, the tolerable crack sizes are determined for a pipe installation procedure which compares the proposed methodology with approach recommended by DNV and benchmark analyses.

2. Strain-based EPRI estimation scheme for homogeneous pipes under bending

The EPRI estimation scheme [15] to estimate the *J*-integral (the procedure to estimate the CTOD is analogous but it is not addressed here in interest of space - readers are referred to the work of Chiodo and Ruggieri [11] for further details) in components containing flaws derives from the fully plastic description of *J* based upon the HRR-controlled crack tip fields [23]. The procedure begins by considering the elastic and plastic contributions to the *J*-integral as

$$J = J_e + J_p \tag{1}$$

where the elastic component, J_e, is given by

$$J_e = \frac{K_I^2}{E'} \tag{2}$$

in which K_I is the (Mode I) elastic stress intensity factor and $E' = E$ or $E' = E/(1-\nu^2)$ whether plane stress or plane strain conditions are assumed with E representing the (longitudinal) elastic modulus.

For an elastic-plastic material obeying a Ramberg-Osgood model [24,25] to describe the uniaxial true stress ($\bar{\sigma}$) vs. logarithmic strain ($\bar{\epsilon}$) response given by

$$\frac{\bar{\varepsilon}}{\varepsilon_{ys}} = \frac{\bar{\sigma}}{\sigma_{ys}} + \alpha\left(\frac{\bar{\sigma}}{\sigma_{ys}}\right)^n \tag{3}$$

where α is a dimensionless constant, n defines the strain hardening exponent, σ_{ys} and $\varepsilon_{ys} = \sigma_{ys}/E$ define the yield stress and strain, the plastic component, J_p, is expressed as

$$J_p = \alpha\varepsilon_{ys}\sigma_{ys}b\left[h_1\left(\frac{a}{t}, \frac{D_e}{t}, \theta, n\right)\right]\left(\frac{M}{M_0}\right)^{n+1} \tag{4}$$

where D_e is the pipe (cylinder) outer diameter, t is the wall thickness, $b = t - a$ defines the uncracked ligament, M_0 is the limit load of the cracked pipe configuration, M denotes the applied bending moment and the surface crack length is described by the angle θ (see Fig. 3) as

$$\theta = \frac{c}{R_e} \tag{5}$$

where c is the circumferential crack half-length and $R_e = D_e/2$. In the above expression, h_1 is a dimensionless factor dependent upon crack size, component geometry and strain hardening properties of the material. The previous solution for J_p became widely known as the EPRI methodology [15].

Parise et al. [14] have further modified this methodology by writing J_p as a function of applied strain in the structure. Under fully plastic conditions, the first term in the right-hand side of Eq. (3) vanishes, so the Ramberg-Osgood can be reduced to the form

$$\frac{\bar{\varepsilon}}{\varepsilon_{ys}} = \alpha\left(\frac{\bar{\sigma}}{\sigma_{ys}}\right)^n. \tag{6}$$

By noting in the above expression that $\sigma \propto \alpha\varepsilon^{\frac{1}{n}}$, it is possible to rewrite Eq. (4) to express J_p as a function of the applied plastic strain in the component, ε_p, as

$$J_p = \alpha\varepsilon_{ys}\sigma_{ys}b\left[g_1\left(\frac{a}{t}, \frac{D_e}{t}, \theta, n\right)\right]\left(\frac{\varepsilon_p}{\varepsilon_{ys}}\right)^{\frac{n+1}{n}} \tag{7}$$

where g_1 is now the dimensionless factor that relates the plastic component of the J-integral with the applied global plastic strain. This fracture parameter can be determined from an extensive set of 3-D numerical analyses conducted on circumferential surface part-through cracks in the girth weld of pipes or cylinders under bending load with varying crack configuration and material properties, as described in Section 5.1. The plastic strain, ε_p, required by Eq. (7) to the J-integral calculation is determined by subtracting the elastic portion from the total applied strain:

$$\varepsilon_p = \varepsilon - \varepsilon_e \tag{8}$$

in which the total strain can be computed by the pipe outer diameter and the reel drum radius, R_b, by

$$\varepsilon = \frac{D_e/2}{R_b + D_e/2}. \tag{9}$$

The elastic component of the applied strain is simply obtained by dividing the total stress acting on the structure by the elastic modulus, E. This stress quantity can be found by conversion of the remote strain using the stress-strain curve and the Ramberg-Osgood model [14]. Finally, the elastic component of the J-integral is calculated by using Eq. (2) with a convenient solution of K_I for a circumferential surface crack in a pipe subjected to a (pure) bending moment [26].

3. The equivalent stress and strain relationship method (ESSRM)

Lei and Ainsworth [16,17] proposed a simplified J estimation procedure based on an equivalent stress and strain relationship method (ESSRM) in which the effects of weld strength mismatch and weld geometry can be represented by an equivalent stress-strain curve. The J-integral estimation can then be performed by traditional methods for homogeneous materials, such as the EPRI methodology [15]. The weld strength mismatch is defined as the ratio between the yield stress of the weld and the base material as

$$M_y = \sigma_{yw}/\sigma_{yb} \tag{10}$$

where σ_{yw} and σ_{yb} are the yield stress of the weld and base material respectively. The equivalent stress-strain relationship, σ_{eq}, is defined as:

$$\sigma_{eq}(\varepsilon_p) = f_1\sigma_{wm}(\varepsilon_p) + f_2\sigma_{bm}(\varepsilon_p) \tag{11}$$

where $\sigma_{eq}(\varepsilon_p)$ denotes the equivalent stress-plastic strain relationship, f_1 and f_2 define functions of the weld joint geometry and mismatch ratio, which can be determined from convenient limit load analyses of the structure. The stress-plastic strain relationship of the weld metal is defined by

$$\frac{\varepsilon_p}{\varepsilon_{yw}} = \alpha_w\left(\frac{\sigma}{\sigma_{yw}}\right)^{n_w}, \tag{12}$$

and for the base metal

$$\frac{\varepsilon_p}{\varepsilon_{yb}} = \alpha_b\left(\frac{\sigma}{\sigma_{yb}}\right)^{n_b}. \tag{13}$$

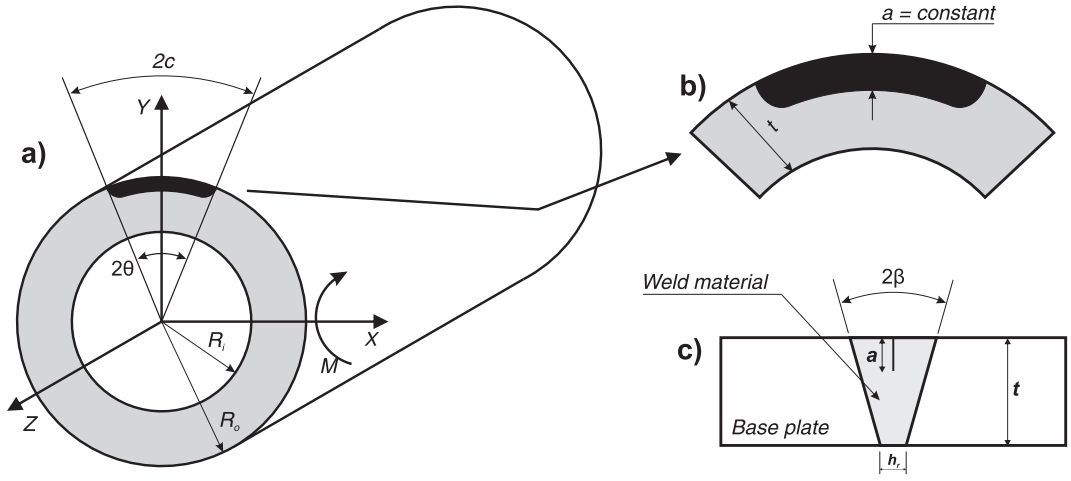

Fig. 3. Schematic illustration of the pipe configuration: (a) pipe and crack geometry, (b) detail of the crack region and (c) weld groove geometry.

When both materials have the same strain hardening coefficient ($n_b = n_w$), the equivalent stress-strain curve obtained by the ESSRM is simply described by an equivalent strain hardening exponent $n_{eq} = n_b = n_w$ [9,16,27].

Now, following Lei and Ainsworth [16], the equivalent yield stress for the welded structure is given by

$$\sigma_{ye} = \frac{P_0^{mism}}{P_0^{bm}}\sigma_{yb} \tag{14}$$

where P_0^{mism} denotes the limit load of the idealized bi-material welded joint and P_0^{bm} represents the limit load for the homogeneous component with the base material properties. Limit load solutions for mismatched cracked structures can be determined either by analytical methodologies (slip-line theory) [28] or by finite elements analyses [29].

In summary, the estimation of CDF in mismatched structures consisted by materials with the same strain hardening is simplified into the following steps:

1. Calculate an equivalent material yield strength by applying adequate limit load solutions for the welded structure containing a defect.
2. Calculate the equivalent strain hardening coefficient.
3. Apply an appropriate CDF estimation procedure available to homogeneous structures in the new equivalent material.

In this study, the strain-based version of the EPRI approach will be employed to estimate the CDF in homogeneous pipes, as previously described in Section 2. Substituting the equivalent material properties (σ_{ye} and n_{eq}) in Eq. (7), the modified EPRI equation can be written as

$$J_p = \alpha_e \varepsilon_{ye}\sigma_{ye} b\left[g_1\left(\frac{a}{t}, \frac{D_e}{t}, \theta, n_{eq}\right)\right]\left(\frac{\varepsilon_p}{\varepsilon_{ye}}\right)^{\frac{n_{eq}+1}{n_{eq}}} \tag{15}$$

where $\varepsilon_{ye} = \sigma_{ye}/E$.

Actual flow properties of welded structures depend on a number of variables, such as heat input, welding process, consumable materials, among others. These factors have an strong impact on both yield stress and strain hardening of the weld metal. This work addresses only cases where materials have the same strain hardening coefficient and mismatch in the yield stress. The objective of this simplification is to reduce the numbers of variables involved in the analysis, in order to allow a better understanding of the problem and the controlling factors that influence the procedure accuracy.

4. Numerical procedures and material models

4.1. Finite element models for pipeline girth welds with weld centerline cracks

The finite element models are constructed through a mesh generator developed with Python and the finite element software Abaqus 6.12 [30]. It allows the creation of pipe models with different crack geometries, weld groove and clad layer configurations. Fig. 4 shows a typical finite element model constructed for the pipe with $D_e/t = 10$, $\theta/\pi = 0.12$, $a/t = 0.3$.

The crack is modeled with a rectangular shape and constant depth through the entire crack length, as represented in Fig. 3(b) [12,13]. A conventional mesh configuration having a focal mesh with ten concentric rings of elements surrounding the crack tip is used with the smallest element dimension being on the order of 10^{-2} mm. The crack tip is modeled with collapsed wedge elements which makes the crack ideally sharp initially, but allows it to blunt as deformation advances [14]. To adequately capture the discontinuity effect of the crack, the pipe models were designed with a total length $L = 3D_e$. Due to symmetry, only one quarter of the pipe is modeled with appropriate constraints imposed on the nodes defining the symmetry planes. Typical models have between 15,000 to 30,000 elements and between 30,000 and 45,000 nodes, depending on the crack configuration and pipe geometry.

Pipeline girth weld is explicitly modeled in the finite element analyses by considering a weld root width $h_r = 5$ mm and a V-weld groove angle, as showed in Fig. 4(c). Because the effects of the heat affected zone are not addressed in the present study, the weld strength mismatch is introduced by simply defining different material properties for the weld and base metals.

Hexaedrical eight node isoparametrical elements with reduced integration and hourglass control (C3D8R) were employed in this work. The J-integral is evaluated from the average of the values extracted from each of the ten rings of elements at the deepest point of the crack ($X = 0$), excluding the highly deformed elements of the first ring. Confidence in the mesh refinement was gained through evaluation of the path independence of the numerical values of the J-integral extracted from each ring. The difference between each value and the average is less than 5% and, therefore, the J values are considered accurate. Pure bending moment is applied in the pipe configuration through a rotational displacement at a reference point located at the end of the pipe, as depicted in Fig. 4(a). The nodes at the end of the pipe are connected to the reference point using a multipoint constraint which distributes linearly the displacement originated from the applied rotation. The global strain, ε, applied in the pipe can be directly related to the imposed rotation by the following equation [14]:

$$\varphi = \frac{2L\varepsilon}{D_e} \tag{16}$$

where φ is the angle of rotation imposed in the reference point and L is the pipe length. The total bending moment in each step of the simulation is calculated from the sum of the contributions of each node located in the crack plane.

4.2. Computation of g_1-factors for J estimation

This section describes the analysis matrix employed in the calculation of the g_1-factors applicable to the calculation of the J-integral from Eq. (7). Parise et al. [14] have developed similar analysis to semi-elliptical cracks. However, the present pipe models consider a crack with a constant depth through the entire length, which changes the CDF at the crack tip [13]. Nonlinear 3-D finite element analyses are conducted on circumferentially cracked pipeline girth welds with external surface flaws at the weld centerline subjected to bending. The analyzed pipe models have wall thickness $t = 20.6$ mm with different outside diameters: $D_e = 206$ mm ($D_e/t = 10$) and $D_e = 412$ mm ($D_e/t = 20$).

Three normalized crack lengths are considered in the analyses: $\theta/\pi = 0.04, 0.12$ and 0.20, which correspond to a/c ratios in the range $0.0125 \leqslant a/c \leq 0.625$. The crack depth varies from $a/t = 0.1$ to 0.5 with increments of 0.1. These geometries typify current trends in high pressure, high strength pipelines, including submarine pipelines and risers.

Three different materials are utilized in the analyses: $n = 5$ and $E/\sigma_{ys} = 800$ (high hardening material), $n = 10$ and $E/\sigma_{ys} = 500$ (moderate hardening material), $n = 20$ and $E/\sigma_{ys} = 300$ (low hardening material). All materials have the same elastic properties: $E = 206$ GPa and $\upsilon = 0.3$. The constitutive model follows a flow theory with conventional Mises plasticity in small geometry change (SGC) setting [11]. Above, it is readily understood that

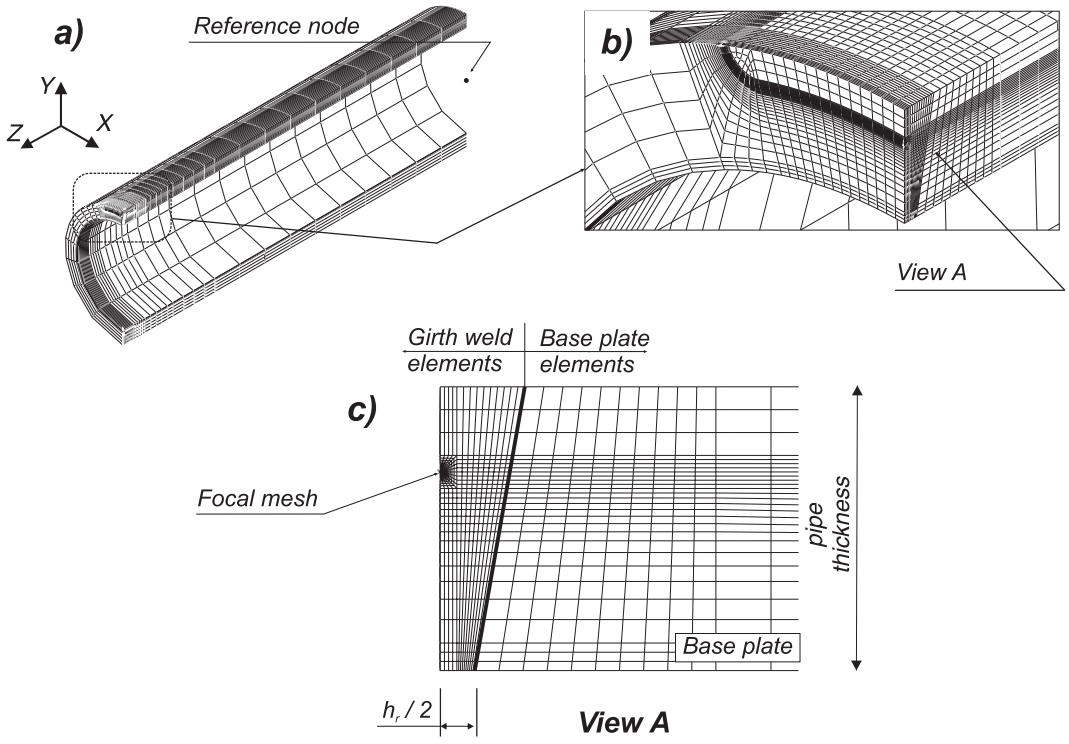

Fig. 4. Typical finite element model employed in the numerical analyses: (a) representation of the pipe mesh and the location of the reference node, (b) detail of the crack region and (c) detail of the weld region and focused mesh configuration around the crack tip.

the α coefficient of the Ramberg-Osgood model is set equal to unity for all materials. The elastic-plastic analyses utilize a simple power-hardening model to characterize the uniaxial true stress ($\bar{\sigma}$) *vs.* logarithmic strain ($\bar{\epsilon}$) in the form

$$\frac{\bar{\epsilon}}{\epsilon_{ys}} = \frac{\bar{\sigma}}{\sigma_{ys}}, \quad \epsilon \leqslant \epsilon_{ys}; \quad \frac{\bar{\epsilon}}{\epsilon_{ys}} = \left(\frac{\bar{\sigma}}{\sigma_{ys}}\right)^n, \quad \epsilon > \epsilon_{ys} \tag{17}$$

where σ_{ys} and ϵ_{ys} are the reference (yield) stress and strain, and n is the strain hardening exponent.

4.3. Parametric validation analyses

Verification analyses were conducted on circumferentially cracked pipes with constant wall thickness $t = 20.6$ mm and outer diameters $D_e = 206$ mm and $D_e = 412$ mm ($D_e/t = 10$ and $D_e/t = 20$). The crack geometry considers two crack lengths ($2c$) and crack depths (a). The normalized crack length is taken as $\theta/\pi = 0.04$ and $\theta/\pi = 0.2$, whereas the crack depth is varied from $a/t = 0.1$ to $a/t = 0.3$.

This investigation considers weld geometries with the same root width $h_r = 5$ mm and two groove angles: $\beta = 30^\circ$ and $\beta = 10^\circ$. They are representative of typical manual and automatic welding procedures (see Fig. 5 for more details about the weld groove configuration).

The verification considers elastic-plastic materials with moderate ($n = 10$ and $E/\sigma_{ys} = 500$) and low hardening properties ($n = 20$ and $E/\sigma_{ys} = 300$). A typical level of undermatch $My = 0.9$ is employed in all analyses and the same strain hardening coefficient is adopted for base and weld metal, as already discussed in Section 3.

5. Results and discussion

5.1. Factors g_1 for circumferential surface cracks in pipes under bending

Factor g_1 is the key parameter for the J-integral estimation procedure outlined in Section 2. Calculation of g_1 follows from rearranging Eq. (7) as

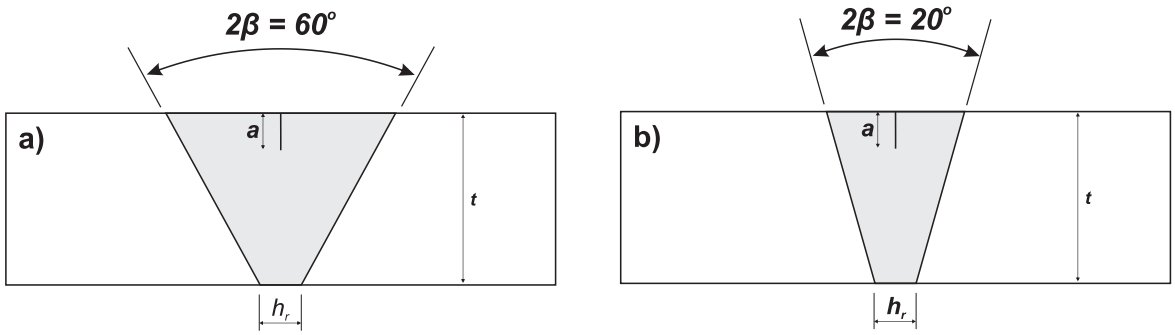

Fig. 5. Illustration of the weld bevel geometries adopted in this work: (a) wide gap weld with $\beta = 30^\circ$ and (b) narrow gap weld with $\beta = 10^\circ$.

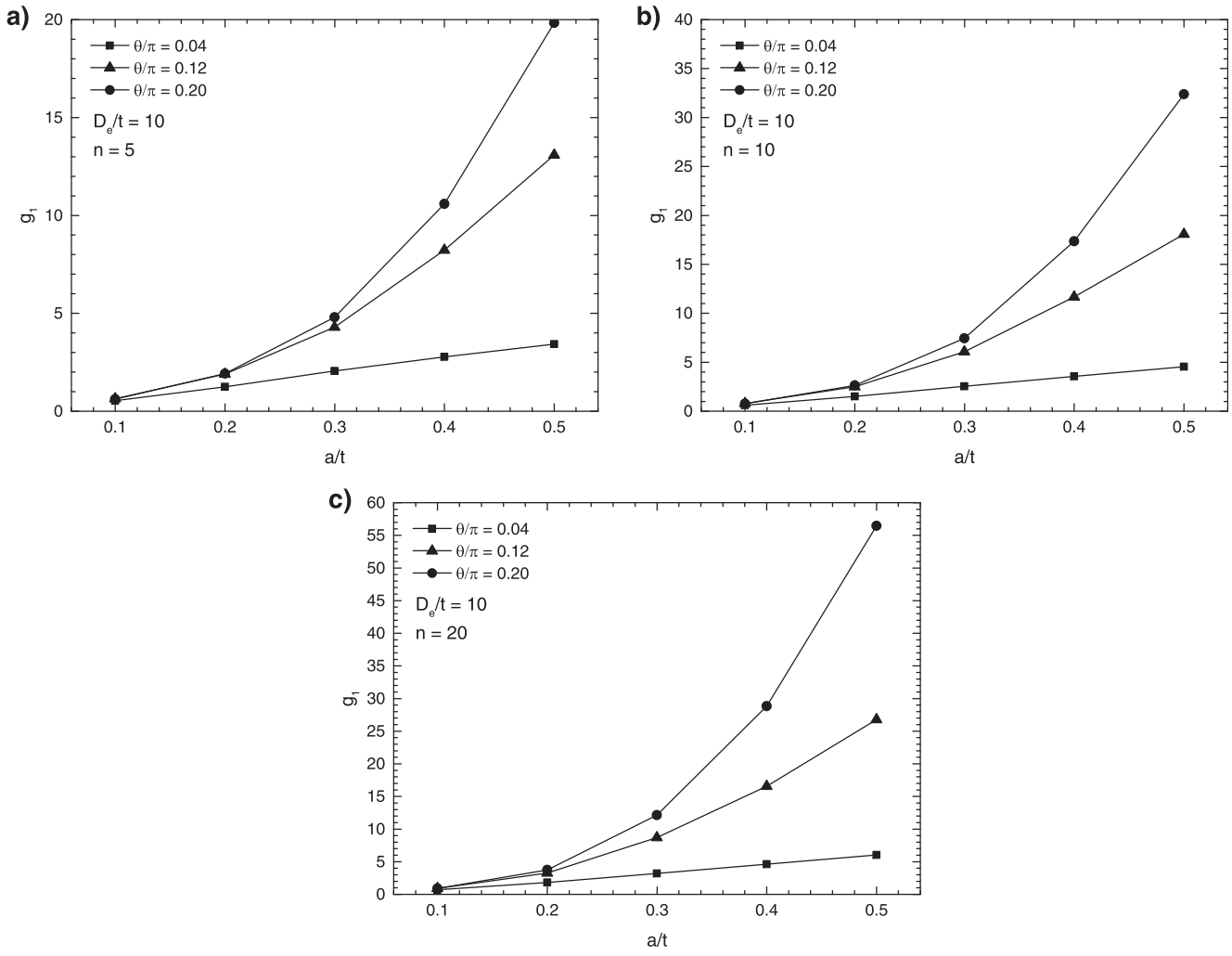

Fig. 6. Variation of factor g_1 with increased a/t-ratio for the pipe configuration with $D_e/t = 10$ and varying circumferential crack length and hardening properties.

$$g_1 = \frac{J_p}{\alpha \varepsilon_{ys} \sigma_{ys} b \left(\frac{\varepsilon_p}{\varepsilon_{ys}}\right)^{\frac{n+1}{n}}} \tag{18}$$

where J_p is obtained by subtracting the elastic component from the total J determined through the finite element analysis. Then, the g_1-factor can be interpreted as the slope of the best fit straight line passing through the axis origin. The fitting procedure excludes points corresponding to strain levels $\varepsilon < \varepsilon_{ys}$ and $\varepsilon > 0.04$ which corresponds to unrealistic high strain levels [14]. The linear regression procedure for all cases presented a coefficient of determination (R-squared) greater than 0.98.

Figs. 6 and 7 provide the g_1-factors for circumferential surface cracks in pipes under bending, for the analysis matrix described in Section 4.2. For all set of analysis, the results reveal that factor g_1 displays a strong sensitivity to the strain hardening level (observe that the scales in the y-axis are different depending on the strain hardening exponent). It can be noted that g_1-factors exhibit a relatively strong dependence on the D_e/t-ratio and crack length (as characterized by θ/π) for moderate to deep crack sizes ($0.25 \leqslant a/t \leq 0.4$) and are almost insensitive to the D_e/t-ratio in the shallow crack size range ($0.1 \leqslant a/t \leq 0.2$). Similar conclusion were drawn by Parise et al. [14]. To provide a simpler manipulation of the results depicted in Figs. 6 and 7, a functional dependence of factor g_1 on crack depth for a given D_e/t and θ/π-ratio and strain hardening, n, is constructed in the form

$$g_1 = \xi_0 + \xi_1(a/t) + \xi_2(a/t)^2 + \xi_3(a/t)^3. \tag{19}$$

Tables 1 and 2 provide the polynomial coefficients resulting from a standard least square fitting to the g_1 data obtained through finite element analyses.

5.2. Crack driving force estimations

The accuracy of crack driving forces estimation in cracked pipeline girth welds plays a key role in integrity assessment of reeled pipes. This section examines the effectiveness of a strain-based version of the EPRI methodology coupled with the ESSRM (see Sections 2 and 3) to adequately describe the evolution of J-integral with applied strain.

The precise determination of limit loads for the mismatched structure are also necessary to the application of the ESSRM [27]. This work adopts the limit load solution for pipes with finite circumferential part-through surface internal cracks at the girth weld subjected to tension load [29], presented in the Appendix. Souza et al. [31] have demonstrated that application of this solution in connection with a weld geometry simplification procedure is adequate to describe the actual component limit load for mismatch levels within ±20%.

The weld groove simplification is constructed based upon the slip-line theory and the similarity between the crack tip constraint of single edge notched tension, SE(T), specimens and pipes with

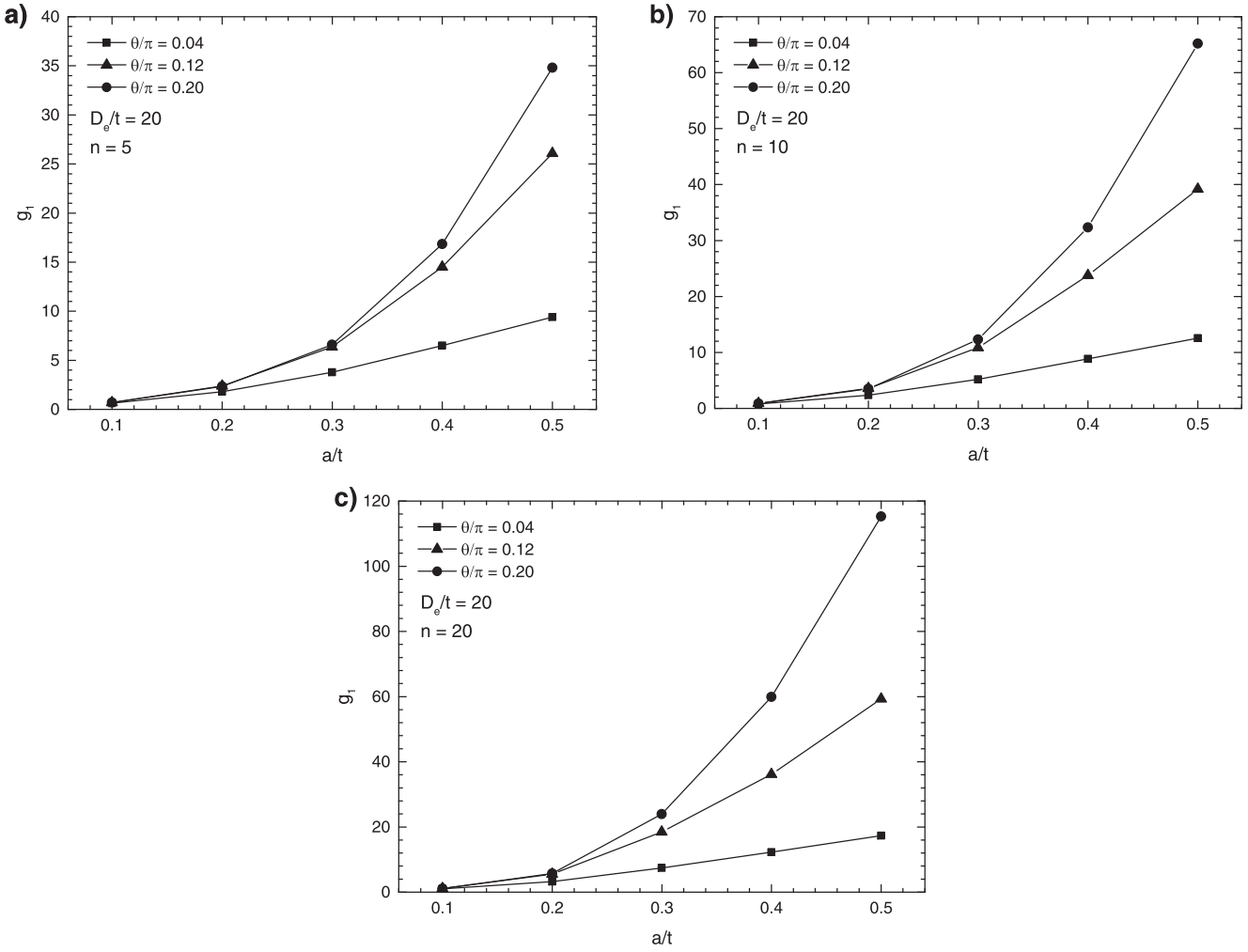

Fig. 7. Variation of factor g_1 with increased a/t-ratio for the pipe configuration with $D_e/t = 20$ and varying circumferential crack length and hardening properties.

Table 1
g_1-factors for a pipe with $D_e/t = 10$ and distinct crack geometries and material strain hardening levels.

n	θ/π	ξ_3	ξ_2	ξ_1	ξ_0
5	0.04	−12.450	9.792	5.205	−0.067
	0.12	−19.217	79.695	−10.751	0.955
	0.20	154.980	−5.330	3.170	0.215
10	0.04	−15.125	14.707	5.654	−0.083
	0.12	−86.575	159.430	−25.567	1.851
	0.20	183.110	59.745	−13.555	1.368
20	0.04	−24.042	26.676	4.758	−0.004
	0.12	−59.467	183.650	−27.122	1.851
	0.20	440.780	16.976	−8.017	1.120

Table 2
g_1-factors for a pipe with $D_e/t = 20$ and distinct crack geometries and material strain hardening levels.

n	θ/π	ξ_3	ξ_2	ξ_1	ξ_0
5	0.04	−50.433	75.674	−7.870	0.728
	0.12	94.675	85.885	−17.469	1.536
	0.20	423.540	−105.490	17.268	−0.386
10	0.04	−96.925	123.950	−14.894	1.143
	0.12	−176.460	380.900	−78.211	5.167
	0.20	557.670	9.878	−17.988	2.065
20	0.04	−140.550	172.620	−19.132	1.318
	0.12	−257.610	533.670	−95.077	5.542
	0.20	486.740	413.600	−113.630	7.874

external surface cracks at the girth weld under bending [32,33]. Assuming that a straight slip-line emanates from the crack tip at an angle of 45° and taking into account that the limit load of a structure is directly related to the length of the slip-line in each material zone, the V-groove can be simplified to a square weld bevel whose width (h_{eq}) is calculated from the intersection between the weld fusion line and the slip-line trajectory as illustrated in Fig. 8 (see Souza et al. [31] and Hertelé et al. [9] for further details).

The verification study is performed by comparing the J-integral predictions obtained from the estimation scheme developed in this work and benchmark solutions using three-dimensional numerical analyses of pipes containing the exact V-weld groove, pipe and crack geometries. It is worth mentioning that the comparisons performed in this study provide useful information only to asses the accuracy of the equivalent stress and strain relationship method and the weld groove simplification.

Prediction of crack driving forces follows from applying the strain-based version of EPRI with the material properties obtained through the equivalent stress-strain curve in Eq. (14) and the limit load results presented in the Appendix. Calculation of the J-integral for a pipe with a V-groove weld was performed by the following steps:

1. Determine the equivalent square groove weld width, h_{eq}, based on the weld groove simplification procedure detailed above and discussed in detail by Souza et al. [31];
2. Calculate the limit load ratio P_0^{mism}/P_0^{bm} using the limit load solution for pipes with finite circumferential part-through surface internal cracks at the girth weld subjected to tension load [29];
3. Calculate the equivalent yield stress, σ_{ye}, from Eq. (14);
4. Calculate the suitable g_1-factor according to the pipe configuration, crack geometry and the equivalent strain hardening coefficient ($n_{eq} = n_b = n_w$) using Eq. (19) and the coefficients from Tables 1 and 2.
5. Calculate the plastic J-integral using Eq. (15) and the equivalent metal properties.

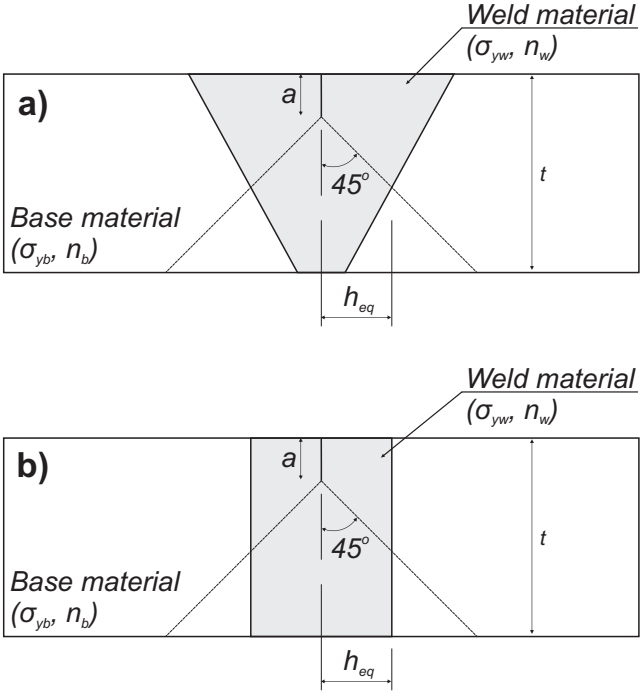

Fig. 8. Weld bevel simplification scheme for a pipeline girth weld without a clad layer.

Fig. 9(a) shows the equivalent stress-strain curve obtained for a pipe with $D_e/t = 20$, $\theta/\pi = 0.04$, $a/t = 0.1$ and a V-groove weld angle, $\beta = 10°$. The analysis considers a base metal with yield stress, $\sigma_{ys} = 412$ MPa and a mismatch level $M_y = 0.9$. Weld and parent metal have the same strain hardening coefficient $n_w = n_b = 10$. The evolution of J_p with applied plastic strain, ε_p, is depicted in Fig. 9(b). For this specific case study, the J_p estimation using the strain-based EPRI coupled with the ESSRM agrees very well with the finite element solutions.

To provide systematic overview of the procedure accuracy, Figs. 10 and 11 depict the ratio between CDF predictions obtained by the method developed in this work and finite element analysis ($J_p^{Eq.\ (15)}/J_p^{FEA}$) with increased applied strain.

Consider first the results shown in Fig. 10(a) for pipe configurations with $D_e/t = 10$, $\theta/\pi = 0.04$, $a/t = 0.1, 0.3$ and girth weld geometries with $\beta = 10°$ and $\beta = 30°$. The predicted crack driving forces (strain-based EPRI) are within 10% of the finite element results for the entire range of applied plastic strain for the weld with a narrow gap geometry and within approximately 15% for the wide gap weld. Note, however, that the estimation accuracy increases with the evolution of applied load. Consider, for example, the shallow crack pipe ($a/t = 0.1$) with $\beta = 10°$. The error in J_p prediction varies from 10% at a plastic strain level of $\varepsilon_p = 0.015$ to 4% for $\varepsilon_p = 0.035$. The same behavior is observed for the other cases.

The weld groove geometry plays an important role in J_p estimations. For all cases covered in this study, application of the procedure in narrow gap welds $\beta = 10°$ results in better agreement to the finite element analyses than the wide gap configuration. The weld fusion line angle in narrow gap welds is small, and thus the weld geometry approaches very closely the rectangular shape required by the limit load solution [29]. Therefore, there is little influence of the weld geometry simplification procedure in converting a V-groove weld to a square shape in the case of a narrow gap weld [31].

The effect of strain hardening is also illustrated in Figs. 10 and 11, which cover the $n = 10$ and $n = 20$ materials respectively. The J_p estimations display a good agreement to the finite element analyses for pipes with narrow gap welds and $n_{eq} = 10$, as the error in predictions are lower than 10% for plastic strain levels $\varepsilon_p > 0.02$ (Fig. 10). However, application of the procedure for materials with high hardening exponents ($n = 20$) results in estimations errors within 15% for narrow gap weld joints and plastic strain levels $\varepsilon_p > 0.02$, as showed in Fig. 11. A somewhat larger difference in CDF predictions occurs for pipes with low hardening materials ($n = 20$) and wide gap weld geometries. For these cases the estimations are within 30%.

5.3. Tolerable crack size estimates for pipes with undermatched girth welds

To verify the effectiveness of the methodology previously developed, this section presents additional analyses with predictions of tolerable flaw sizes for a typical pipeline with a narrow V-groove girth weld and dissimilar material properties [3]. The analyzed pipe has outside diameter $D_e = 203.2$ and steel pipe thickness $t = 20$ mm. The liner/clad thickness is not addressed in the present case study. The material of the pipe is an API 5L Grade X70 pipeline steel with yield stress, $\sigma_{yb} = 551$ MPa, tensile strength, $\sigma_{uts} = 660$ MPa and relatively low hardening properties ($\sigma_{uts}/\sigma_{yb} = 1.20$). According to Annex F of API579 [7], the Ramberg-Osgood strain hardening coefficient describing the stress-strain response of the base metal is $n_b = 14.2$. The weld metal has yield stress, $\sigma_{yb} = 495$ MPa, which is representative of corrosion resistant alloys, such as nickel-chromium alloy 625

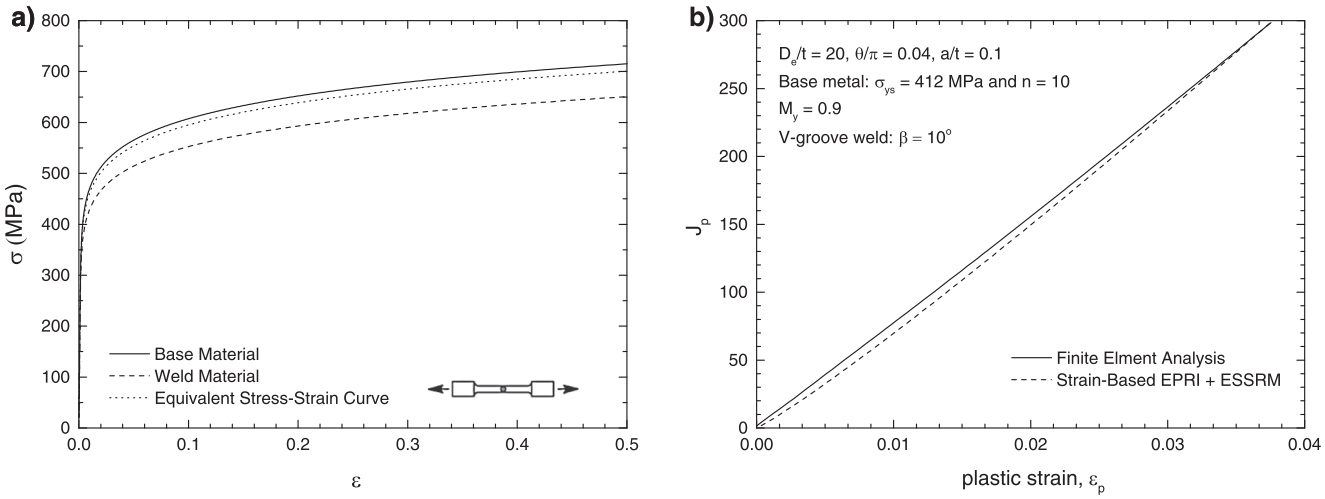

Fig. 9. (a) Illustration of (a) the equivalent stress-strain curve and (b) the evolution of J_p with applied plastic strain, ε_p, for a pipe with a V-groove weld ($\beta = 10^{\circ}$) and mismatch level $M_y = 0.9$.

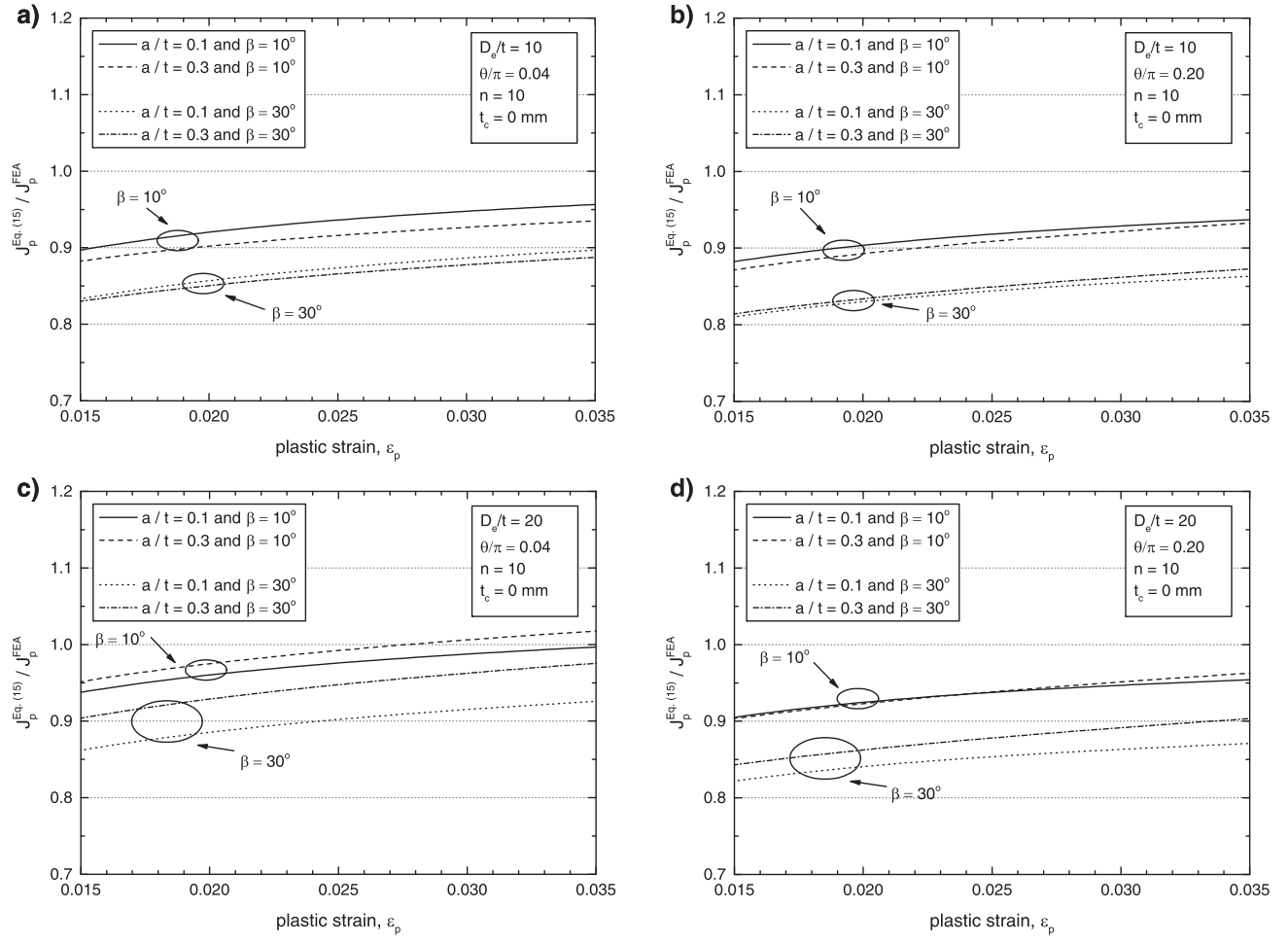

Fig. 10. Comparison between the evolution of J_p *vs.* applied plastic strain obtained through the Strain-based EPRI and finite element analyses for a pipe with weld strength mismatch $M_y = 0.9$ and strain hardening coefficient $n = 10$.

[34]. As described in previous sections, this study considers only idealized situations where both weld and parent metal have the same strain hardening behavior. Thus, the strain hardening coefficient for the weld metal is $n_w = n_b = 14.2$ and the weld strength mismatch level is $M_y = 0.89$. A narrow gap weld is adopted in this case study, as it represents typical automatic welding processes.

Evaluation of tolerable crack sizes in pipe girth welds requires fracture toughness data, usually obtained through testing of small-scale specimens, such as SE(T) (single edge notched tensile) [35,36]. This work adopts the J-value at onset of crack growth defined by $J = 400\,\mathrm{kJ/m^2}$ as the material's elastic-plastic toughness, J_{mat}. This toughness value is typical for Alloy

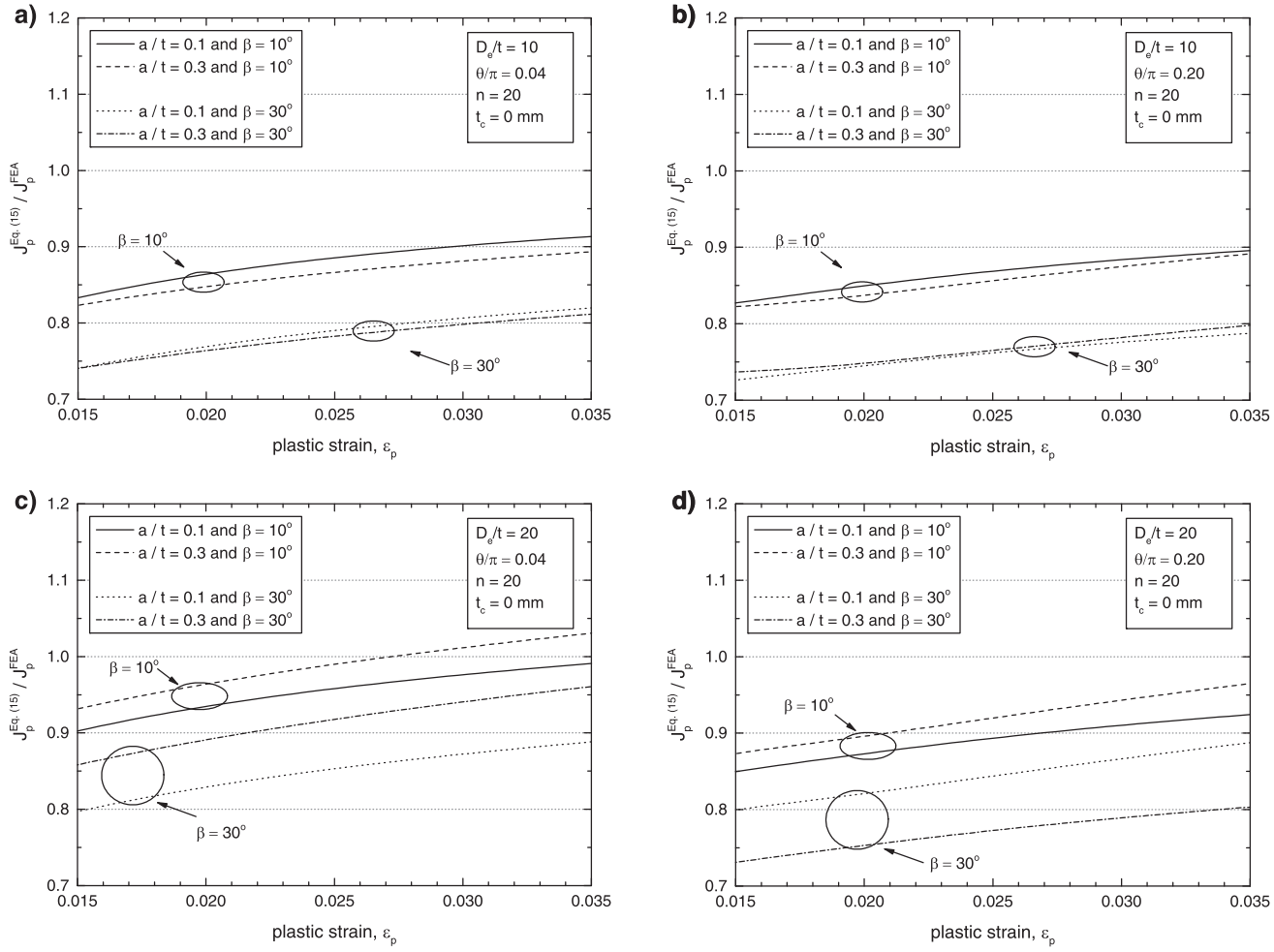

Fig. 11. Comparison between the evolution of J_p *vs.* applied plastic strain obtained through the Strain-based EPRI and finite element analyses for a pipe with weld strength mismatch $M_y = 0.9$ and strain hardening coefficient $n = 20$.

625 materials, including weld metal and heat affected zone region [3].

The maximum applied strain level can be directly evaluated from the geometry of reel drum and the pipeline, as described in Eq. (9). This work adopts a strain level $\varepsilon = 0.02$ for the analyses and prediction of critical flaws.

Results obtained through the methodology developed in this work are compared with two related procedures: (a) 3D finite element analysis of the actual pipeline and girth weld configuration and (b) the DNV approach, which is based on the BS7910 [6] and the reference stress [37] with limit load solutions taken from Kastner et al. [38] and stress intensity factors from Raju and Newman [39]. Because 3D finite element models represent very closely the pipeline and girth weld geometry, the numerical results are considered here as benchmark solutions and provide a basis of comparison to the other procedures.

The framework to calculate the critical crack sizes at dissimilar girth weld follows the structure presented in Section 5.2 with minor changes. For a fixed crack length, $2c$ and varying crack depth a, the calculation of critical flaw sizes is performed by the following steps:

1. Determine the weld strength mismatch level M_y, using Eq. (10);
2. Determine the equivalent square groove weld width, h_{eq} for the correspondent crack depth a value [31];
3. Calculate the limit load ratio P_0^{mism}/P_0^{bm} using the limit load solution for pipes with finite circumferential part-through surface internal cracks at the girth weld subjected to tension load [29] and presented in Appendix A;
4. Calculate the equivalent yield stress, σ_{ye}, from Eq. (14);
5. Calculate the suitable g_1-factor according to the pipe configuration, crack geometry and the equivalent strain hardening coefficient ($n_{eq} = n_b = n_w$) using Eq. (19) and the coefficients from Tables 1 and 2.
6. Calculate the plastic J-integral using Eq. (15) and the equivalent metal properties.
7. Calculate the elastic component of the J-integral using Eq. (2).
8. Calculate the total J-integral ($J = J_e + J_p$) and compare the obtained crack driving force with the critical toughness value (J_{mat}).
9. Repeat the procedure until the $J > J_{mat}$ is satisfied and determine the critical crack depth

Fig. 12 shows the tolerable crack sizes obtained for a pipe reeling procedure in which the maximum strain applied in the pipe is $\varepsilon = 0.02$ and the material toughness is $J = 400$ kJ/m^2. Critical flaws are presented in terms of the critical crack depth, a, and fixed crack lengths, $2c = 50, 75$ and 100 mm.

For short cracks, $2c = 50$ mm, the strain-based version of EPRI methodology coupled with the ESSRM overestimate the critical

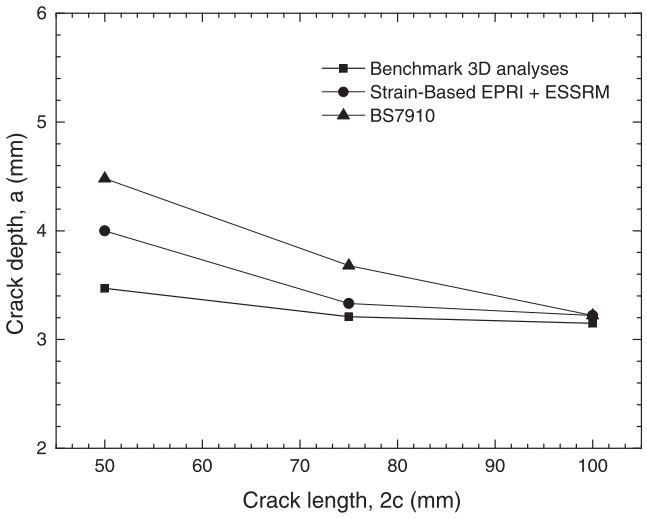

Fig. 12. Tolerable crack size comparison.

crack depth with a deviation of 15% in relation to the benchmark 3D analyses. However, the overestimation is even more pronounced for the BS7910 procedure, as the tolerable crack depth is about 30% greater than the corresponding value predicted by the strain-based methodology proposed in the present work. A similar trend is observed for the crack length $2c = 75$ mm. While application of the procedure developed in this work results in differences of 4% with respect to the 3D analyses, BS7910 overestimates the tolerable crack sizes by 15%. For long cracks, there is little difference in critical crack size estimations and differences are within 2%. While predictions with the new methodology shows a slight deviation from the benchmark, it is possible to conclude that there will be a gain in accuracy when compared to the DNV approach, which recommends BS7910.

Similar error levels were reported by Pepin et al. [4] for pipes with undermatched girth welds. Hertelé et al. [9] have verified that the fracture response of simplified welds are slightly nonconservative and proposed a safety factor to correct the estimations in order to apply the method to structural integrity assessments.

Safety factors can be calculated directly from the crack driving force estimations performed in Section 5.2, so the predictions obtained from Eq. 15 match the J_p extracted from finite element analysis ($J_p^{Eq.\ (15)} = J_p^{FEA}$). Consider, for instance, the analyses for a material with yield stress $\sigma_{ys} = 412$ MPa, strain hardening coefficient $n_b = 10$ and mismatch level $M_y = 0.9$, as presented in Fig. 10. For a plastic strain $\varepsilon_p = 0.02$, the maximum deviation in the case of narrow gap welds occurs for a pipe with $D_e/t = 10$, $\theta/\pi = 0.20$, $a/t = 0.3$, $\beta = 10^\circ$, as the ratio $J_p^{Eq.\ (15)}/J_p^{FEA} = 0.89$ (Fig. 10(b)). The safety factor for this case must be 1.12.

Following the procedure above mentioned, the overall safety factor for a plastic strain level $\varepsilon_p = 0.02$ must be 1.17 for pipes with narrow gap welds ($\beta = 10^\circ$), as this value ensures that the prediction will be conservative for the material properties and pipe configurations adopted in this work.

6. Concluding remarks

This work describes a J-integral estimation procedure for fracture assessments of circumferential surface cracks in undermatched pipe girth welds subjected to high levels of bending load. The proposed method derives from a strain-based version of the EPRI J-estimation scheme [14] coupled with the equivalent stress-strain relationship method [16] and a weld bevel simplification scheme [9,31]. The proposed formulation takes advantage of the displacement controlled conditions of the reeling process, so the CDF can be determined without requiring previous knowledge of the applied load on the pipe. Moreover, it takes into account the approximately linear relationship between the plastic strain level and the J-integral which mitigates the impact of any errors in load calculation for cases where load controlled methodologies are applied to estimate the J-integral.

The extensive set of nonlinear, 3D finite element analyses provides the fracture parameters required by the strain-based version of the EPRI methodology, which enters directly into the J-integral estimation of cracked pipes and cylinders subjected to bending load. The application of the equivalent stress-strain relationship method and an appropriate limit load solution allows the representation of the complex coupled effects of weld strength mismatch and weld geometry in a single equivalent stress-strain curve which has approximately the same mechanical response of the welded joint. The J-integral estimation can then be performed by traditional methods for homogeneous materials, such as the strain-based version of the EPRI methodology.

Verification analyses were conducted to assess the procedure accuracy in precisely describing the CDF in surface cracks at the girth weld of reeled pipelines. The parametric analyses reveal that the methodology predicts the CDF with good accuracy for the entire set of pipe configurations and material properties for narrow gap welds. However, when the methodology is applied to wide gap joints and low hardening materials the differences in J-estimation are within 30% which raises concern about the direct application of the method for such cases without considering a proper safety factor.

Additional analyses were performed to compare the tolerable crack sizes in pipe girth welds subjected to the reeling procedure. The results obtained through the procedure developed in this work were compared with those from the approach recommended by DNV and 3D benchmark analyses. The critical crack sizes obtained by the new method are in close agreement to the benchmark analyses and present a better accuracy when compared to the DNV procedure.

Acknowledgments

The financial support of the Brazilian National Council for the Improvement of Higher Education (CAPES) is gratefully acknowledged. The authors also acknowledge the Brazilian State Oil Company (Petrobras) for providing additional support for the work described here. Helpful discussions with Dr. E. Hippert (Petrobras) are also acknowledged.

Appendix A

Kim et al. [29] describe a limit load expression applicable to pipes with a finite circumferential part-through surface internal cracks at the girth weld subjected to tension, where the slenderness parameter, ψ, is defined as

$$\psi = \frac{t-a}{h} + 5\left(\cos\left(\frac{\theta}{2}\right) - \frac{\sin\theta}{2}\right) \tag{A.1}$$

in which t is the pipe wall thickness and h denotes the square weld strip width. The crack is defined by its depth, a, and circumferential angle 2θ. The limit load ratio (N_0^{mism}/N_0^{bm}) for overmatched girth welds is determined by

$$\frac{N_0^{mism}}{N_0^{bm}} = \begin{cases} \min\left(M_y, \frac{1}{n_{LB}}\right) & 0 \leqslant \psi \leqslant \psi_1 \\ \min\left(\frac{24(M_y-1)}{25}\left(\frac{\psi_1}{\psi}\right) + \frac{(M_y+24)}{25}, \frac{1}{n_{LB}}\right) & \psi_1 \leqslant \psi \end{cases} \tag{A.2}$$

$$\psi_1 = \exp\left(-\frac{2(M_y - 1)}{5}\right) \tag{A.3}$$

where N_0^{bm} is defined as the limit tension load of the structure. For undermatched pipes, the limit load ratio is defined by:

$$\frac{N_0^{mism}}{N_0^{bm}} = \begin{cases} M_y & 0 \leqslant \psi \leqslant 1.5 \\ 1 - \frac{1.5(1-M_y)}{\psi} & 1.5 \leqslant \psi \end{cases} \tag{A.4}$$

References

[1] S. Kyriakides, E. Corona, Mechanics of Offshore Pipelines, Buckling and Collapse, vol. 1, Elsevier, 2007.

[2] E. Olso, E. Berg, B. Nyhus, C. Thaulow, E. Ostby, A new assessment approach for ECA of clad and lined pipes based on shell and line-spring finite elements, in: Proceedings of the Twenty-first (2011) International Offshore and Polar Engineering Conference, 2011.

[3] R.F. Souza, C. Ruggieri, Fracture assessments of clad pipe girth welds incorporating improved crack driving force solutions, Eng. Fract. Mech. 148 (2015) 383–405, https://doi.org/10.1016/j.engfracmech.2015.04.029.

[4] A. Pepin, T. Tkaczyk, N. O'Dowd, K. Nikbin, Methodology for assessment of surface defects in undermatched pipeline girth weld, J. Pressure Vessel Pip. Technol. 137(5). doi:http://dx.doi.org/10.1115/1.4029190.

[5] Det Norske Veritas, Submarine pipeline systems, Offshore Standard OS-F101, 2013.

[6] British Institution, Guide to methods for assessing the acceptability of flaws in metallic structures, BS 7910, 2013.

[7] American Petroleum Institute, Fitness-for-service, API RP-579-1/ ASME FFS-1, 2007.

[8] T. Tkaczyk, N.P. O'Dowd, K. Nikbin, Fracture assessment procedures for steel pipelines using a modified reference stress, J. Pressure Vessel Technol. 131 (3) (2009) 1–11, https://doi.org/10.1115/1.3122769, paper 031409.

[9] S. Hertelé, W.D. Waele, M. Verstrate, R. Denys, N. O'Dowd, J-integral analysis of heterogeneous mismatched girth welds in clamped single-edge notched tension specimens, Int. J. Pressure Vessel Pip. 119 (2014) 95–107.

[10] M. Paredes, C. Ruggieri, Further results in J and CTOD estimation procedures for SE(T) fracture specimens – Part II: Weld centerline cracks, Eng. Fract. Mech. 89 (2012) 24–39.

[11] M.S.G. Chiodo, C. Ruggieri, J and CTOD estimation procedure for circumferential surface cracks in pipes under bending, Eng. Fract. Mech. 77 (2010) 415–436.

[12] E. Ostby, K.R. Jayadevan, C. Thaulow, Fracture response of pipelines subject to large plastic deformation under bending, Int. J. Pressure Vessels Pip. 82 (3) (2005) 201–215.

[13] N. Nourpanah, F. Taheri, Development of a reference strain approach for assessment of fracture response of reeled pipelines, Eng. Fract. Mech. 77 (2010) 2337–2353.

[14] L.F.S. Parise, C. Ruggieri, N. O'Dowd, Fully plastic strain-based J estimation scheme for circumferential surface cracks in pipes subjected to reeling, J. Pressure Vessel Technol. 137 (4) (2015), https://doi.org/10.1115/1.4028111, 041204–041204–8.

[15] V. Kumar, M.D. German, C.F. Shih, An engineering approach to elastic-plastic fracture analysis, Tech. Rep. EPRI NP-1931, Electric Power Research Institute, Palo Alto, CA, 1981.

[16] Y. Lei, R.A. Ainsworth, A J integral estimation method for cracks in welds with mismatched mechanical properties, Int. J. Pressure Vessel Pip. 70 (1997) 237–245.

[17] Y. Lei, R.A. Ainsworth, The estimation of J in three-point-bend specimens with a crack in a mismatched weld, Int. J. Pressure Vessel Pip. 70 (1997) 247–257.

[18] E. Ostby, Fracture control offshore pipelines: new strain based fracture mechanics equations including the effects of biaxial loading, mismatch and misalignment, in: International conference on offshore mechanics and arctic engineering OMAE, Halkidiki, Greece, 2005.

[19] Y.M. Zhang, Z.M. Xiao, W.G. Zhang, On 3-D crack problems in offshore pipeline with large plastic deformation, Theoret. Appl. Fract. Mech. 67–68 (2013) 22–28.

[20] N. Bonora, A. Carlucci, A. Ruggiero, G. Ianniti, Fracture integrity assessment of flawed bi-metallic girth weld joint, in: ASME 2013 Pressure Vessels and Piping Conference, Paris, France, 2013.

[21] N. Bonora, A. Carlucci, A. Ruggiero, G. Ianniti, Simplified approach for fracture integrity assessment of bimetallic girth weld joint, in: ASME 2013 32nd International Conference on Ocean, Offshore and Arctic Engineering, Nantes, France, 2013.

[22] M. Paredes, C. Ruggieri, Engineering approach for circumferential flaws in girth weld pipes subjected to bending load, Int. J. Pressure Vessel Pip. 125 (2015) 49–65.

[23] J.W. Hutchinson, Fundamentals of the phenomenological theory of nonlinear fracture mechanics, J. Appl. Mech. 50 (1983) 1042–1051.

[24] T.L. Anderson, Fracture Mechanics: Fundaments and Applications, third ed., CRC Press, Boca Raton, FL, 2005.

[25] N.E. Dowling, Mechanical Behavior of Materials: Engineering Methods for Deformation, Fracture and Fatigue, second ed., Prentice Hall, New Jersey, 1999.

[26] A. Zahoor, Ductile fracture handbook, Tech. Rep. EPRI NP-6301-D, Electric Power Research Institute, Palo Alto, CA, 1989.

[27] Y. Lei, J. Tao, P.N. Li, Limit load and J estimates of a centre cracked plate with an asymmetric crack in a mismatched, Int. J. Press. Vessels Pip. 76 (1999) 747–757.

[28] S. Hao, A. Cornec, K.-H. Schwalbe, Plastic stress-strain fileds and limit loads of a plane strain cracked tensile panel with a mismatched welded joint, Int. J. Solids Struct. 34 (1997) 297–326.

[29] J.-S. Kim, T.-K. Song, Y.J. Kim, T.-E. Jin, Strength mismatch effect on limit load for circumferential surface cracked pipes, Eng. Fract. Mech. (2009) 12.

[30] Dassault Systémes Simulia Corp., ABAQUS Standard - V. 6.12, Providence, RI, USA, 2012.

[31] R.F. Souza, C. Ruggieri, Z. Zhang, A framework for fracture assessments of dissimilar girth welds in offshore pipelines under bending, Eng. Fract. Mech. 163 (2016) 66–88, https://doi.org/10.1016/j.engfracmech.2016.06.011.

[32] D.F.B. Sarzosa, C. Ruggieri, A numerical investigation of constraint effects in circumferentially cracked pipes and fracture specimens including ductile tearing, Int. J. Pressure Vessel Pip. 120–121 (2014) 1–18.

[33] B. Nyhus, M. Polanco, O. Ørjasæter, SENT specimens as an alternative to SENB specimens for fracture mechanics testing of pipelines, in:22nd International Conference on Ocean, Offshore and Arctic Engineering (OMAE) , Vancouver, Canada, 2003.

[34] American Society for Testing and Materials, Standard specification for nickel-chromium-molybdenum-columbium alloy (UNS N06625) and nickel-chromium-molybdenum-silicon alloy (UNS N06219) plate, sheet, and strip, ASTM B443-00, 2009.

[35] S. Cravero, C. Ruggieri, Estimation procedure of J-resistance curves for SE(T) fracture specimens using unloading compliance, Eng. Fract. Mech. 74 (2007) 2735–2757.

[36] Det Norske Veritas, Fracture control for pipeline installation methods introducing cyclic plastic strain, DNV-RP-F108, 2006.

[37] R.A. Ainsworth, The assessment of defects in structures of strain hardening material, Eng. Fract. Mech. (1984) 19.

[38] W. Kastner, E. Röhrich, W. Schmitt, R. Steinbuch, Critical crack sizes in ductile piping, Int. J. Pressure Vessel Pip. 9 (1981) 197–219.

[39] I.S. Raju, J.C. Newman, Stress intensity factors for a wide range of semi-elliptical surface cracks in finite thickness plates, Eng. Fract. Mech. 11 (4) (1979) 817–829.